Structure and Stability of Aluminum Alkyl Cocatalysts in Ziegler−Natta Catalysis

Antulio Tarazona and Eckhard Koglin

Institute of Applied Physical Chemistry (IPC), Research Center Jülich, D-52425 Jülich, Germany

Francesco Buda

INFM-FORUM, Scuola Normale Superiore, Piazza dei Cavalieri 7, I-56126 Pisa, Italy

Betty B. Coussens, Jaap Renkema, Sef van Heel, and Robert J. Meier*

DSM Research, P.O. Box 18, 6160 MD Geleen, The Netherlands

Received: December 6, 1996; In Final Form: March 26, 1997[⊗]

The structure of organoaluminum(halide) complexes, used as cocatalysts in Ziegler−Natta catalysis, is investigated by experimental far-infrared spectroscopy and by quantum simulations. Experimental and calculated far-infrared spectra agree very well, holding promise for the employed far-infrared/quantum simulation approach to reveal more detail on the catalytically active site in Ziegler−Natta catalysis. Whereas the species preferably form dinuclear aluminum complexes when the bridge can be formed by chlorine, on the basis of the calculated total energies and the observed infrared spectra, alkyl-bridged dimers are found to be much less stable.

1. Introduction

Whereas, worldwide, recent research on olefin polymerization is very much focused on the use of metallocene catalysts, practically all of the current production processes run with the traditional Ziegler−Natta or Phillips-type catalysts. It is, however, not clear to what extent the classical catalysts will be overtaken by metallocene catalysts. Consequently, research on Ziegler−Natta and Phillips-type catalysts remains opportune. Moreover, from a scientific point of view, and though Ziegler−Natta catalysis is now over 40 years of age,[1] well-established detailed knowledge on the mechanism of olefin polymerization using these catalysts is still lacking. One of the traditional mechanisms employed to describe the insertion and polymerization of α-olefins is the mechanism proposed by Cossee.[2] Regarding the new metallocene catalysts for olefin polymerization, which can be much more easily subjected to molecular simulation because of their uniquely defined molecular structure, recent high-level quantum mechanical simulations[3−6] primarily seem to plead in favor of the Brookhart-Green mechanism.[7] Because of the much less well-defined geometrical structure and chemical composition of the active site, the structural features of the Ziegler−Natta catalysts at the molecular level are far less well understood. In order to elucidate details of the mechanism of Ziegler−Natta catalysis, we anticipate that experimental spectroscopy studied in conjunction with theoretical analysis will provide a more sound basis for the understanding of the mechanisms involved in Ziegler−Natta catalysis. The use of quantum mechanically simulated spectra for the elucidation of the active site, regarding intermediates in Ziegler−Nata catalysis, has been reported before,[8] but no comparison with experimental spectra was provided.

In the present paper, we report on the far-infrared spectra of organoaluminum(halide) complexes used as cocatalysts in Ziegler−Natta catalysis. These systems were deliberately chosen because they are particularly relevant to Ziegler−Natta catalysis. The complexity of these systems is sufficient to evaluate the applicability of a combined far-infrared/quantum simulation approach for future application to the actual Ziegler−Natta-type catalytic sites involving Ti or V. Whereas the spectra of the aluminum alkyl compounds may be recorded straightforwardly using a modern FT-IR spectrometer equipped with a far-IR option, it is the interpretation of the spectra, including both vibrational frequencies and intensities, which is the primary target of the current investigation. If the current approach based on a mutual comparison of measured and simulated far-infrared spectra allows for sufficient discrimination between different species, as well as identification based on a comparison to simulated spectra, a method would be available which may subsequently be employed to study and characterize the Ti and V sites in Ziegler−Natta systems.

It has been often argued that the aluminum alkyl cocatalyst is present in dimeric form.[9,10] Depending on the presence of chlorine, the bridge might be formed either by alkyl or by chlorine. The stability of the Al_2Me_6 dimeric form was even measured in the gas-phase, with an enthalpy of dimerization close to 20 kcal/mol in favor of the dimeric form.[10] Proton magnetic resonance experiments of the species in toluene or cyclopentane have been argued to agree with the presence of the dimeric form.[10] Tri*ethyl*aluminum, however, was found less strongly dimerized than tri*methyl*aluminum in the vapor phase, but was strongly associated in solution by 17 kcal/mol as measured in hexadecane (for reference to the original works see those quoted in ref 10). On the other hand, very strong dependence of dimer concentration both on absolute concentration of the aluminum-alkyl species and on temperature has also been reported.[11] Whereas these studies report strong association of trimethylaluminum even in the vapor phase, at low pressure and high temperature the monomeric form dominates.[10−13] In conclusion, there seems no straightforward answer to the degree of dimerization from an experimental point of view, and the degree of association seems at least strongly dependent on environment and on temperature.

Infrared spectra of aluminum-alkyls have been reported by Hoffmann[14] and Onishi and Shimanouchi.[15] The latter authors only recorded the spectra of Al_2Me_6 and Al_2Et_6. Hoffmann

* Author to whom correspondence should be addressed.
[⊗] Abstract published in *Advance ACS Abstracts,* May 1, 1997.

S1089-5647(96)03999-5 CCC: $14.00

reported both the infrared and the Raman spectra of a substantial number of aluminum alkyls and aluminum dialkylchlorides, but not the far-infrared part which is of interest with respect to the present study. Hoffmann arrived at an interpretation of the spectra while referring to the well sought spectrum of diboran B_2H_6.[14] Onishi and Shimanouchi have accomplished spectrum interpretation by performing a normal mode analysis involving a Urey−Bradley force field. These studies have provided a satisfactory description of the normal modes of vibrations of several of the aluminum alkylchlorides. However, it is our (future) goal to employ the far-infrared spectra to establish the structure of catalytically active species. Consequently, we need to be able to describe the infrared spectrum in sufficient detail in order to arrive at identification. The methods of analysis employed in the previous studies[14,15] have been suitable for describing the vibrational frequencies and were regarded as state-of-the-art in former days. Full quantum mechanical calculations are today more feasible see, e.g., the work on monomeric and dimeric magnesium dichloride by Molnár et al.,[16] and may include the calculation of both the vibrational frequencies and the vibrational intensities. The results of such a series of calculations relating to the far-infrared spectra of aluminum alkylchlorides will be presented in the current paper.

In order to evaluate the stability of the dimeric forms, the energies of the monomers have been calculated next to the dimer energies. Because the computational demand increases strongly with the size of the molecule, we started calculations with the methyl group as a ligand. Infrared spectra were recorded on available methyl containing aluminum alkyls and compared to the calculated spectra. A more restricted set of aluminum ethyl species was subjected to computation of the far-infrared spectra. In both cases, i.e., methyl and ethyl ligand, it was investigated to what extent the combination of experiment and theory leads to the unique identification of the various species.

In addition, in order to evaluate the stabilibity of the bridged species at finite temperature, quantum molecular dynamics simulations were performed in order to evaluate the stability of some of the bridged species.

2. Experimental Details

2.1. Materials. The aluminum methyl compounds were obtained from Aldrich Chemie in the form of 1.0 M solutions in "hexanes" for all chloride containing Al compounds and as a 2.0 M solution in heptane for trimethylaluminum. The aluminum−ethyl compounds were obtained from WITCO, and solutions were "homemade" in *n*-hexane. The most suitable (on basis of the overall transmission in each spectrum) spectra were obtained when the $AlMe_3$ was measured as a 2 M solution in hexane, whereas all other species were dissolved in hexane with a concentration which was roughly 0.3 M.

2.2. Infrared Spectra. Far-infrared spectra have been recorded on a Perkin−Elmer system 2000 FT-infrared spectrometer system equipped with a far-IR module. A grid beamsplitter (aluminized film) was employed. The source was a wire coil operated at about 1350 K, whereas a far-infrared DTGS detector with a polyethylene window was used. All other windows in the system including the sample vessel were polyethylene. The spectral range covered in our measurements was 700−50 cm^{-1}, the resolution was 4 cm^{-1}, while the number of scans was typically 500. All spectra shown in this paper were difference spectra, i.e., the spectrum of the *n*-hexane solvent has been subtracted.

The simulated spectra shown in this paper were prepared with the GRAMS package, using Lorentzian line shapes. The peak widths were constant and set to 10 cm^{-1} for the methylaluminum species. Because the experimental spectra showed a much larger variation in line width for the ethylaluminum species, the line widths for the individual bands in the spectra of these species have been adapted to the experimental line-widths, under the condition that the integrated intensity of each band is kept as (ab initio) calculated.

TABLE 1. Dimerization Energies for the Aluminum methylchlorides. Numerical Data Originate from the Present Hartree−Fock Energies

dimer	constituing monomers	dimerization energy (kcal/mol)
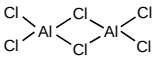	$AlCl_3$, $AlCl_3$	−18.3
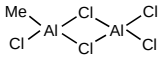	$AlCl_2Me$, $AlCl_3$	−18.8
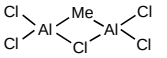	$AlCl_2Me$, $AlCl_3$	−6.3
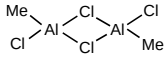	$AlCl_2Me$, $AlCl_2Me$, $AlCl_3$, $AlMe_2Cl$	−18.6 −23.7
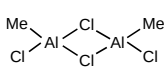	$AlCl_2Me$, $AlCl_2Me$	−18.0
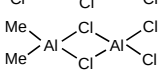	$AlMe_2Cl$, $AlCl_3$	−21.0
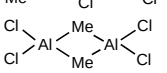	$AlCl_2Me$, $AlCl_2Me$	+1.2
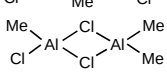	$AlCl_2Me$, $AlMe_2Cl$	−19.4
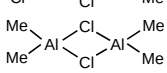	$AlMe_2Cl$, $AlMe_2Cl$	−19.2
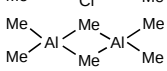	$AlMe_3$, $AlMe_3$	−2.8

2.3. Computational Details. *2.3.1. Hardware.* Hartree−Fock calculations were performed on the CRAY YMP-4 at the Research Center Jülich. The Car−Parrinello calculations were run on an IBM RISC 3CT workstation with 256 MByte RAM at DSM Research.

2.3.2. Software. The Hartree−Fock calculations were carried out using the Gaussian 94 program.[17] The software package employed to carry out the Car−Parrinello method type calculations was the Ab-initio Quantum Molecular Dynamics (AIMD) package. This program has resulted from a cooperation between IBM Zürich Research Laboratories (ZRL) and the IBM European Center for Engineering and Scientific Computing (ECSEC, Rome).

2.3.3. Calculational Details. Hartree−Fock calculations involved energy minimization until the individual gradients were less than 5.10^{-4} hartree/bohr and the root-mean-force less than 3.10^{-4} hartree/bohr. Due to concurrently set limits for the maximum displacement and root-mean-square displacement, after minimization the individual gradients were often smaller by an order of magnitude compared to the above-mentioned threshold values. Energy minimization was followed by a vibrational analysis involving the calculation of infrared and Raman frequencies and infrared intensities. A 6-31G* set was employed for all atoms, whereas a 6-31G** basis was used for the methyl group when it is in the bridge of a dimeric aluminum alkyl.

The Car−Parrinello method [18] combines the molecular dynamics simulation with an accurate description of the interatomic potential, which is based on electronic structure calculation. The quantum description of the electronic structure is based on the density functional theory (DFT). The exchange−correlation energy functional in the DFT is treated within the

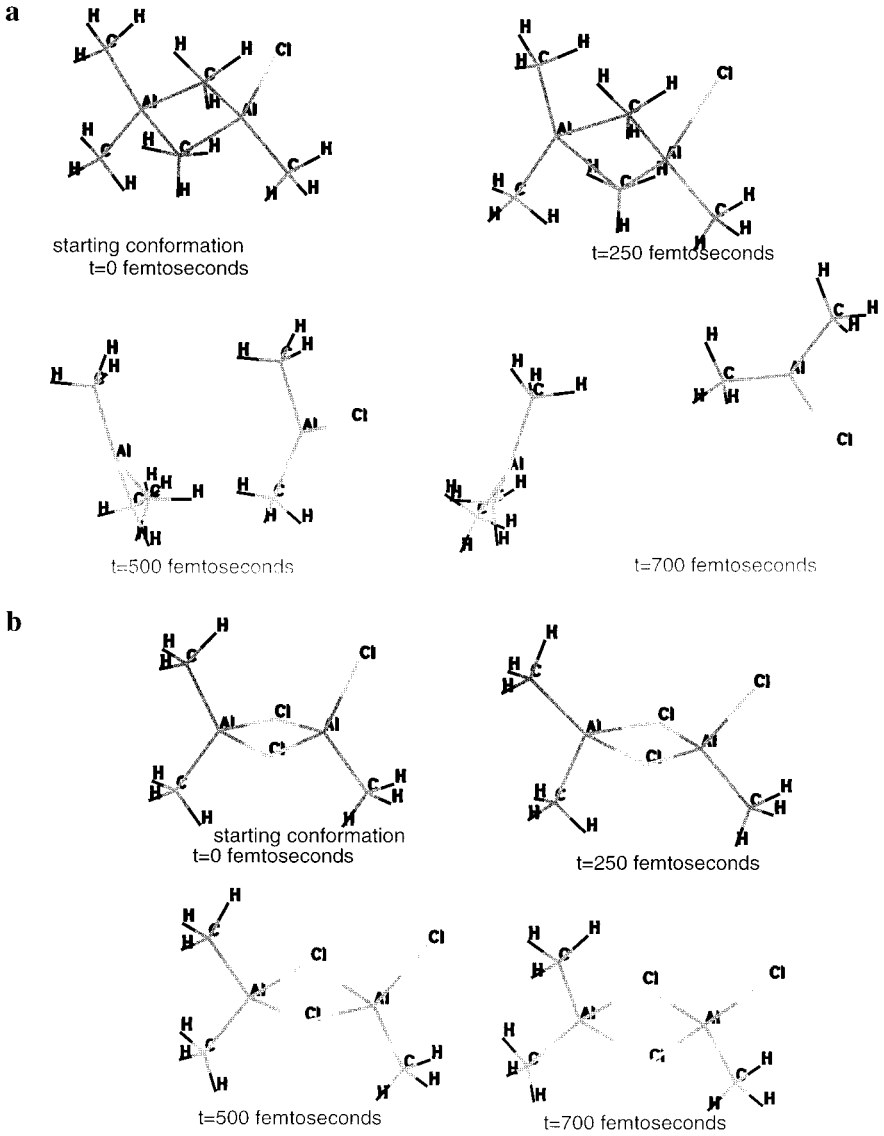

Figure 1. (a) Snapshots taken during the quantum molecular dynamics simulation on $Al_2ClMe_3(Me_2)_{bridge}$ performed at a simulation temperature of $T = 400$ K. (b) Snapshots taken during the quantum molecular dynamics simulation on $Al_2ClMe_3(Cl_2)_{bridge}$ performed at a simulation temperature of $T = 400$ K.

TABLE 2. Experimental and Calculated Structural Parameters for the Al_2Me_6 Dimer. ED is Electron Diffraction

geometrical parameter	X-ray, Lewis and Rundle[25]	X-ray, Vranka and Amma[26]	gas phase, ED[27]	calculated, present study; Hartree−Fock	calculated, present study; DFT in Car−Parrinello
$Al-C_{bridge}$ (Å)	2.24	2.14	2.14	2.17	2.13
$Al-C_{nonbridge}$ (Å)	2.00	1.96	1.96	1.98	1.95
Al-Al (Å)	2.55	2.60	na[a]	2.64	2.58
$C_{bridge}-Al-C_{bridge}$ (deg)	110	105	na	122	104
$Al-C_{bridge}-Al$ (degrees)	70	75	na	66	74
$C_{nonbridge}-Al-C_{nonbridge}$ (deg)	124	123	na	122	119

[a] na = not available.

local density approximation (LDA) for which we employed the Perdew−Zunger parametrization for the homogeneous electron gas.[19] In addition, gradient corrections were included according to the schemes proposed by Perdew[20] and Becke.[21] In the Car−Parrinello quantum molecular dynamics simulations, the molecules treated had a dimension of some 8 Å on average (referring to all three dimensions) and were placed in a cubic box of 11 Å. Only valence electrons were treated explicitly, while pseudopotentials were used to account for the core. Very soft pseudopotentials of the Vanderbilt type were employed,[22] except for Al for which a Bachelet−Hamann−Schlüter type[23] pseudopotential was used. In order to avoid problems in describing the cusp of the hydrogen 1s wave function correctly in a plane−wave expansion, the hydrogen orbital was described by a pseudopotential described by a single Gaussian. The latter pseudopotential has been devised in such a way that it correctly describes the $1/r$ behavior outside the core region. An energy cutoff of 25 Ry was employed for the plane−wave expansion. Before a molecular dynamics simulation was started, a steepest descent energy minimization was performed. The maximum residual gradient after this minimization procedure was less than 10^{-2} hartree/bohr; the majority of the gradients were less than 10^{-3} hartree/bohr. The simulations were performed while keeping the temperature fixed at $T = 400$ K (fluctuations up to 40 K were allowed) by rescaling the atomic velocities. Initial

atomic velocities were generated by rescaling the residual forces acting on each of the atoms after energy minimization.

2.4. Notation for Bridged Species. We need to briefly address on the way of annotating the various species. For the monomers and dimers with only one type of ligand, i.e., only alkyl or only chlorine ligands, the annotation will be sufficiently clear in the text that follows. The way we have annotated the dimers with both alkyl and chlorine ligands requires further explanation. The species $Al_2Cl_4(MeCl)$ has the ligands noted in brackets in the bridge, while the other four ligands are all chlorine atoms. Al_2Me_2-1,4-$Cl_2(Cl_2)$ is the dimer with chlorine atoms in the bridge, while the other four ligands are two chlorine atoms and two methyl groups, the latter in −1,4− position as illustrated in

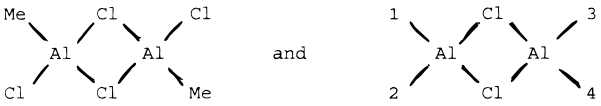

Similarly, for $AlMe_2Cl_4$, there are also the configurations Al_2Me_2-1,2-$Cl_2(Cl_2)$ and Al_2Me_2-1,3-$Cl_2(Cl_2)$, i.e.,

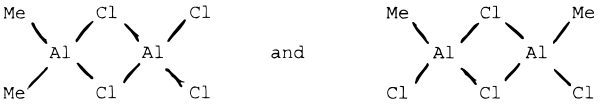

3. Results and Discussion

3.1. Hartree−Fock Energy Calculations. Stability of the Dimeric Form of the Alkylaluminum(halides). Hartree−Fock-calculated minimum energies are supplied in the Supporting Information. Table 1 contains the dimerization energies for the methyl species. From these data is may be directly concluded that formation of a chlorine bridged dimer is energetically strongly favored, whereas this is clearly less so for the methyl-bridged species.

The calculated energy of dimerization for Al_2Cl_6 (18.3 kcal/mol) may be compared to experimental values in the range of 22−29 kcal/mol.[10] The agreement is reasonable in view of the accuracy of both numbers (7 kcal/mol spread in experimental values); moreover, it may be realized that we compare calculated dimerization energies in vacuum with experimental values measured in solution. Whereas the literature is not unequivocal regarding the stability of the trimethylaluminum dimer versus its monomer form (see the Introduction), our calculations reveal a dimerization energy of 2.8 kcal/mol only. Because it might be argued that Hartree−Fock level calculations do not produce sufficiently reliable energetics, we have performed additional simulations at the density functional theory level including gradient corrections. Results obtained from these first principles molecular dynamics simulations of the Car−Parrinello type, aiming to reveal the stability of the dimer at finite temperature, will be discussed in the next subsection. In subsection 3.3 the structure and energetics of the trimethylaluminum species will be further discussed.

3.2. First Principles. Molecular Dynamics (Car−Parrinello) Simulations. The results reported in the previous paragraph suggest that methyl-bridged species, such as Al_2Me_6, are stable with respect to dissociation, but to a considerably less extent than chlorine-bridged species. Because the trimethylaluminum dimer was calculated to be only 2.8 kcal/mol (12 kJ/mol) more stable than the dissociated monomer pair, it might be anticipated that dynamics at higher temperatures, e.g., $T = 400$ K, would lead to dissociation of the dimeric species. In order to reveal the stability of the bridged aluminum−alkyl and aluminum chloride species at finite temperature, we have performed quantum molecular dynamics simulations on $Al_2ClMe_3(Me_2)_{bridge}$ and on $Al_2Cl_3Me(Cl_2)_{bridge}$ at $T = 400$K. The results of these simulations are shown in Figure 1 in the form of snapshots taken during the simulations. From these structures it is clearly seen that the methyl bridged species is unstable at $T = 400$ K, whereas the chlorine-bridged species is stable (evidently we ought to say stable within the time span of the simulation).

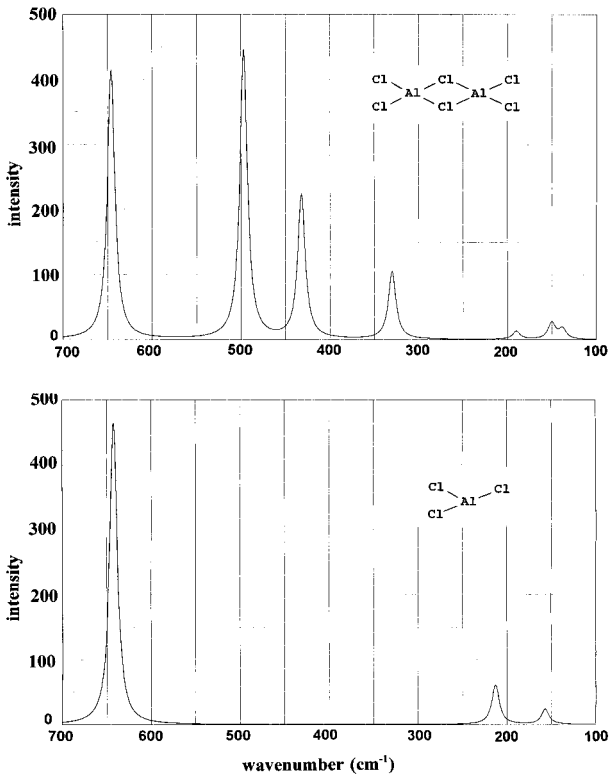

Figure 2. Experimental and computed far-infrared spectra of aluminum trichloride, $AlCl_3$, calculated spectra only.

For organometallics the level of description employed in this calculation, involving a density functional theory description including nonlocal gradient corrections, seems to be recognized as being comparable as the MP2/6-31G** level within the Hartree−Fock scheme (see in particular ref 3 for such comparison regarding ethylene−metallocene complexes, where one may also mutually compare the results presented in refs 3−6, and see also ref 24 for a similar comparison on ethylene−platinumhydride complexes). In addition, density functional level of theory, with nonlocal gradient corrections, included, gives a better account of electron-correlation than the standard Hartree−Fock level of theory. Because electron-correlation effects are expected to be important in systems involving possible bond rupture when the trimethylaluminum dimer dissociates, both the structure and the energetics from the current Car−Parrinello result is considered more reliable than the reported 6-31G*(*) Hartree−Fock results. Consequently, the current Car−Parrinello simulations provide further evidence that also at ambient temperature the degree of dimerization is considerably less than 100% for trimethylaluminum.

3.3. The Structure and Energetics of the Trimethylaluminum Dimer. The stability of the dimer of trimethylaluminum is discussed separately because there is no unequivocal answer to the degree of association as corroborated from existing literature reporting experimental work on this species. Trimethylaluminum has its melting point at 15 °C [11] and its crystal structure has been studied by X-ray diffraction.[25,26] In

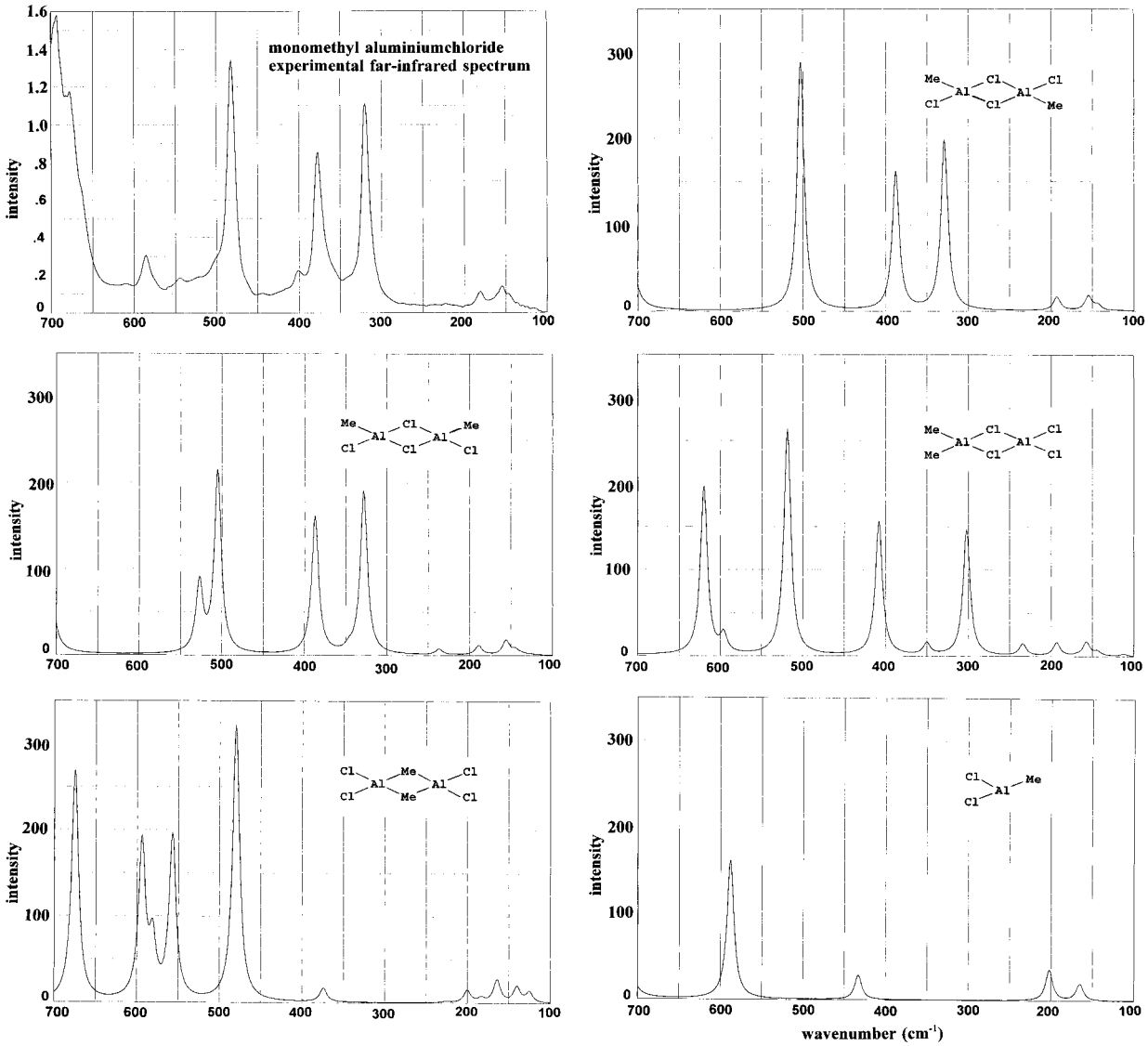

Figure 3. Experimental and computed far-infrared spectra Al_2MeCl_2 and $AlMeCl_2$ isomers.

the crystalline state this species is present in the form of dimers. Some relevant geometrical parameters as obtained from experimental work[25,26] and from our computations have been collected in Table 2. The Hartree−Fock calculations on Al_2Me_6 involved a 6-31G** basis set on the bridging methyl groups and a 6-31G* basis set on the other methyl groups. We conclude from the data presented in Table 2 that the Hartree−Fock calculated and the experimental geometries for Al_2Me_6 agree to a reasonable extent. The effect of the basis set, i.e., the difference between using either a 6-31G* or a 6-31G** basis set, on the C_{methyl}−Al distances was evaluated from calculations on monomers and was found to be less than 0.002 Å. It is also observed that there is no significant difference between the structure of the Al_2Me_6 species in the crystal, as determined by X-ray diffraction and the free molecule structure determined by gas-phase electron diffraction.[27] The structure of the dimethyl-bridged dimer $Al_2Me_3Cl(Me_2)$ obtained from the density functional method as implemented within the Car−Parrinello method yields structural parameters which are in very good agreement with the corresponding experimentally determined parameters for the dimer of $AlMe_3$, as shown in Table 2. Regarding the pure geometrical parameters, the Car−Parrinello (DFT-LDA) result is superior to the current Hartree−Fock calculated structure.

Our calculations suggest that the methyl-bridged species may only be slightly stable with respect to dissociation, which is consistent with some literature data (see the Introduction). For some of the aluminum alkyl species, a strong dependence of the dimerization on (i) temperature, (ii) solvent, and (iii) concentration has been reported on basis of experimental data.[10] For example, the degree of dissociation of liquid triethylaluminum at 20 °C, while dissolved in a hydrocarbon solution in 1% concentration, is only 0.08%. At a concentration in hydrocarbon solution of 0.000 01%, the degree of dissociation has increased to 30%. A simultaneous rise in temperature up to 80 °C (our Car−Parrinello simulations were performed for $T = 127$°C) leads to 95% dissociation (a table with more detailed numbers on these dependencies can be found in ref 10).

In conclusion, the results from our calculations imply a substantial fraction of the monomer being present, which is in accordance with experimental data recorded at low concentration and high temperature. Further evidence for the preference for the monomeric form for trialkyl aluminum species in a specific solution can be obtained from the far-infrared spectra discussed in subsection 3.4.

3.4. Experimental and Computed Far-Infrared Spectra of Aluminum Alkyls. *3.4.1. Aluminum Methyl Species*. We now arrive at what we consider the most essential part of this study in view of our set goal, which is to investigate whether a unique identification of the molecular structure of aluminum alkyls is possible by comparing their experimental and calculated

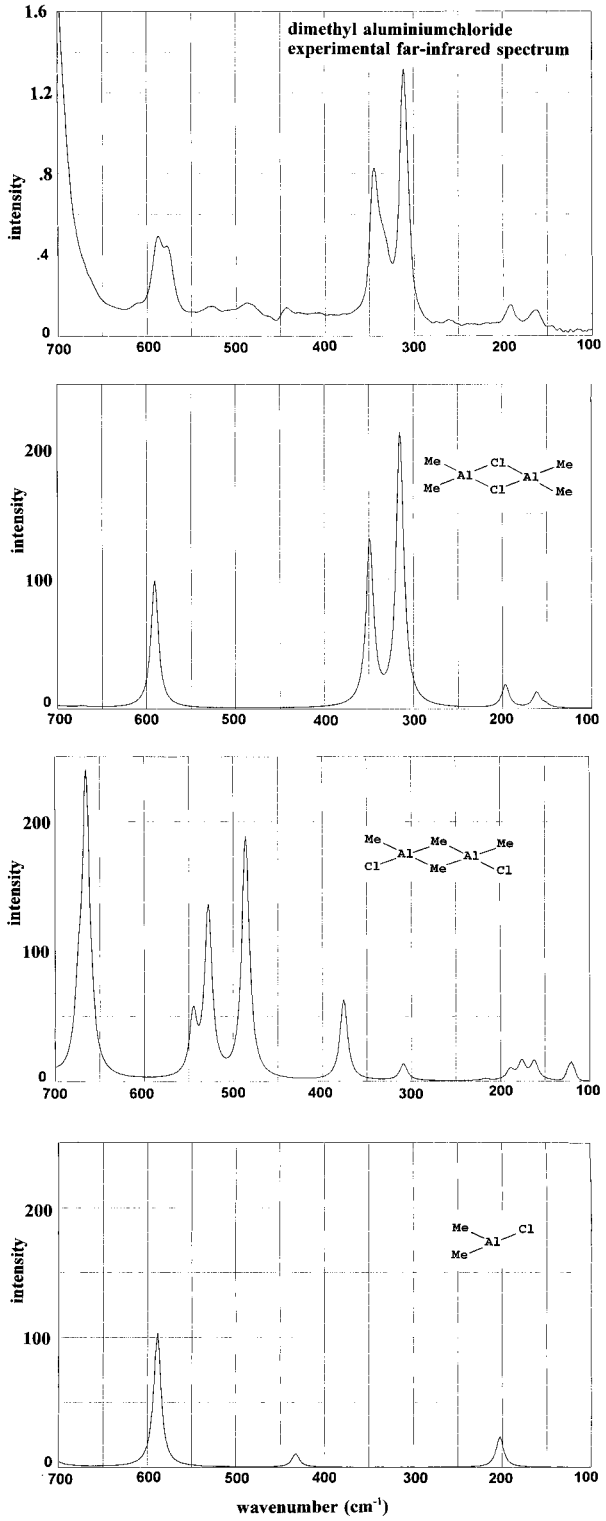

Figure 4. Experimental and computed far-infrared spectra of $Al_2Me_4Cl_2$ and isomers.

far-infrared spectra. The far-infrared spectra are shown in Figures 2−5 for the methyl species and in Figures 6−8 for ethyl-containing species. Only the range 100−650 cm^{-1} will be considered because the range above 650 cm^{-1} is dominated by vibrations due to the methyl groups and possibly suffer from residual interference arising from the solvent (hexane).

Klemperer[28] has recorded the spectrum of gaseous $AlCl_3$. In the far-infrared region he reported absorption bands at 420, 484, and 625 cm^{-1}. Klemperer recorded the spectrum from 1200 down to 325 cm^{-1}, and may therefore just have missed the dimer absorption band calculated at 330 cm^{-1}. The currently presented

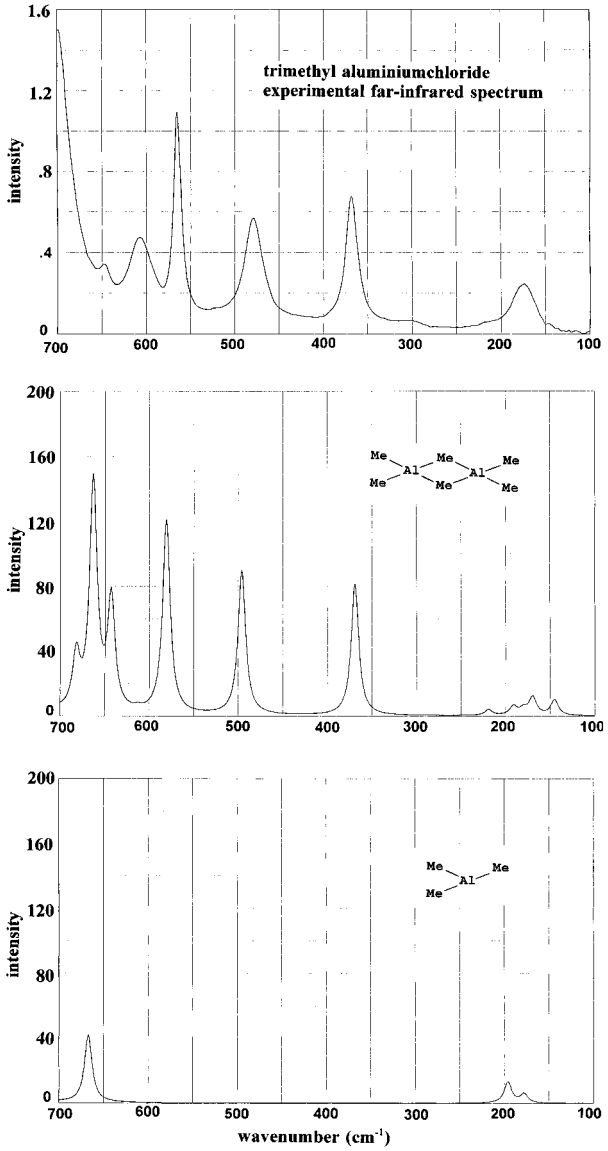

Figure 5. Experimental and computed far-infrared spectra of Al_2Me_6 and AlMe3.

calculated band positions at 432, 497, and 646 cm^{-1} are in very good agreement with the experimental band positions. Moreover, because the calculated spectrum of the $AlCl_3$ monomer does not exhibit bands in this frequency range, the presence of dimers is demonstrated herewith. On the other hand, the absence of vibrational intensity in this frequency range due to the monomer, makes it impossible to estimate the concentration of dimers with respect to monomer concentration. In the 1200−325 cm^{-1} spectral range Klemperer observed but a single band for the monomer $AlCl_3$ centered at 610 cm^{-1}. This is in agreement with our calculated spectrum which reveals a single band at 642 cm^{-1}.

Regarding the methyl-containing dimers, we first consider $Al_2Me_2Cl_4$. The experimental spectrum and the computed spectra for each of the possible dimer configurations have been displayed in Figure 3. The experimental spectrum in the 100−650 cm^{-1} range closely resembles the spectrum of the Al_2Me_2-1,4-Cl_2(Cl_2) dimer. The experimental spectrum also agrees with the spectral features at around 480 and 600 cm^{-1} reported by Groenewege,[29] who recorded the spectral range above 400 cm^{-1} only. These findings are in full agreement with the observations based on the calculation of relative energies suggesting that (i) the dimer is more stable than decomposition into monomers for this chlorine bridged species and (ii) for the various possible

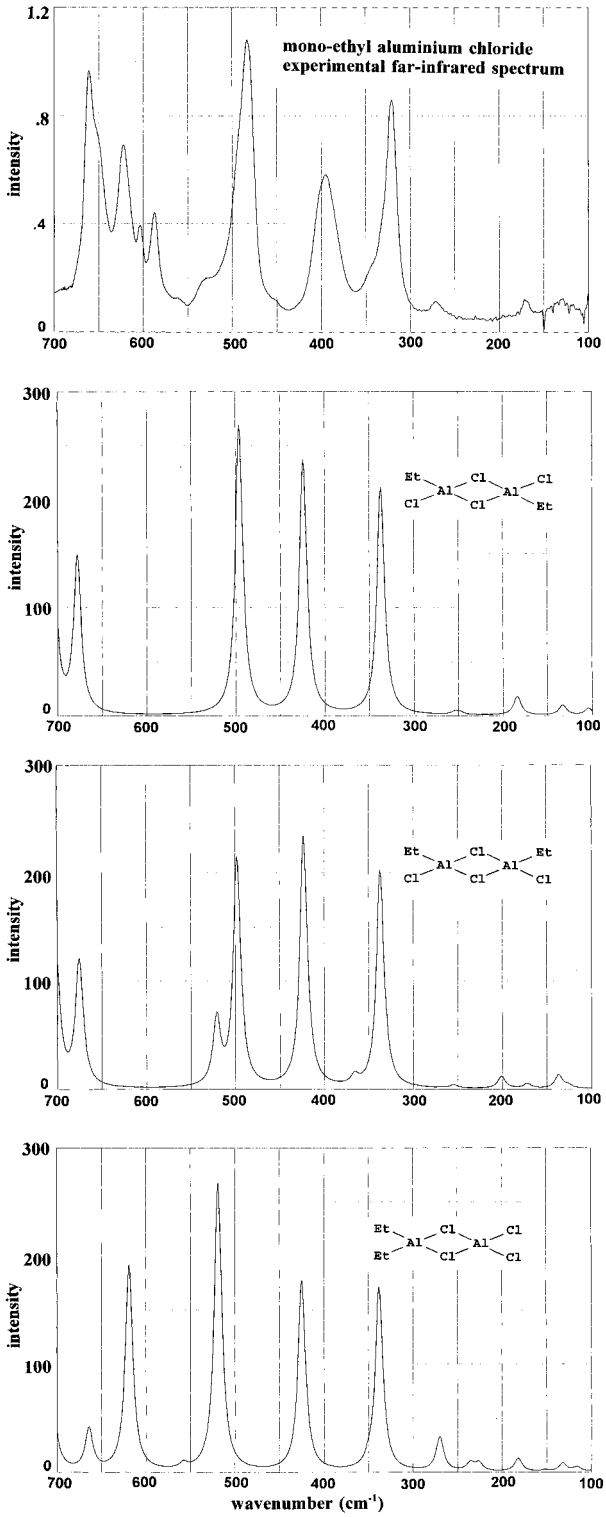

Figure 6. Experimental and computed far-infrared spectra of AlEt2C14. In the computed spectra the line widths have been roughly adapted to the experimental line widths, under the conditions that the integrated intensity of each band is kept as calculated.

$Al_2Me_2Cl_4$ species, the Al_2Me_2-1,4-$Cl_2(Cl_2)$ dimer is the most stable isomer. However, the lower intensity peak near 585 cm^{-1} in the experimental spectrum can be attributed to the presence of the monomer $AlMeCl_2$. Because the calculated maximum intensity for the monomer is only some 50% of the maximum calculated intensity found in the calculated dimer spectrum, the intensity in the experimental spectrum observed near 585 cm^{-1} implies a nonnegligible monomer concentration. It might be surprising to conclude this because we concluded from the

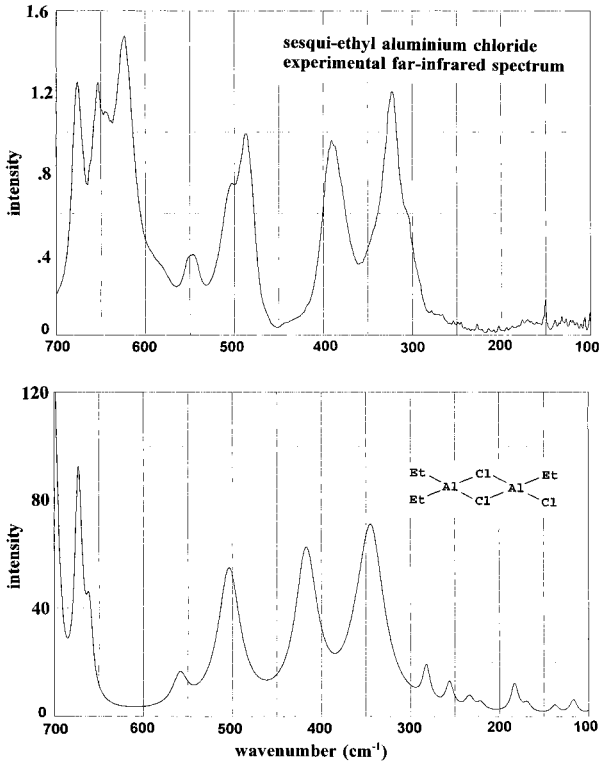

Figure 7. Experimental and computed far-infrared spectra of AlEt3C13. In the computed spectra the line widths have been roughly adapted to the experimental line widths, under the conditions that the integrated intensity of each band is kept as calculated.

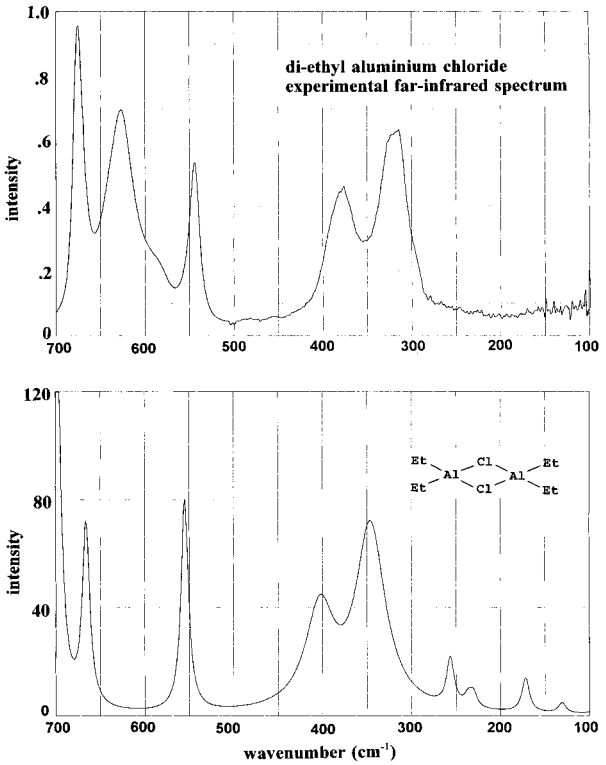

Figure 8. Experimental and computed far-infrared spectra of $AlEt_4Cl_2$. In the computed spectra of the line widths have been roughly adapted to the experimental line widths, under the conditions that the integrated intensity of each band is kept as calculated.

Hartree−Fock calculations that this dimer was more stable than the two corresponding monomers by 18.6 kcal/mol (78 kJ/mol). This possible discrepancy can be explained by the observation that entropy effects tend to largely cancel enthalpy differences, as was likewise reasoned for the case of magnesium chloride.[16]

For the $Al_2Me_4Cl_2$ the observations are very much the same as for the $Al_2Me_2Cl_4$ species. First, the bands reported by van der Kelen,[30,31] and Groenewege[29] at 585 and 720 cm^{-1} were also seen in our spectrum, see Figure 4. Our experimentally observed spectrum closely resembles the calculated spectrum for the dimeric form $Al_2Me_4(Cl_2)$, which is in accordance with energetic considerations, revealing that the chlorine bridged isomer is the most stable one. There seems hardly any intensity which needs to be attributed to a (low) concentration of the monomer $AlMe_2Cl$ (compare with calculated spectrum for $AlMe_2Cl$).

The spectrum of the all methyl species, i.e., $AlMe_3$ and/or its dimer form, shown in Figure 5, is in agreement with the spectrum on the same species presented by Onishi and Shimanouchi.[15] Because of the lack of any significant absorption bands due to the monomer in the spectral range below 650 cm^{-1}, no statements can be made on basis of the frequencies and relative intensities whether a (considerable) fraction of the species is present in the form of monomers. In order to further analyse the situation, and to focus on the relative stability of the Al_2Me_6 dimer versus dissociation, we have compared the experimental absorption intensities of the $AlMe_3$ species and the chloride-containing (bridged) species $AlMeCl_2$ and $AlMe_2Cl$. In the far-infrared region, the absorption intensities of $AlMe_3$ are approximately 1 order of magnitude smaller compared to the absorption intensity for the chlorinated (bridged) species. Because the extinction coefficients for low-frequency, $AlMe_3$ monomer and dimer absorption bands do not differ by more than a factor of 2−3 (as can be corroborated from the calculated intensities displayed along the vertical axes in Figure 5), the 1 order of magnitude difference in absorption intensity between the various aluminimum alkyl species and the $AlMe_3$ solution can only be attributed to a much lower degree of association of the latter. Thus, the relative energies presented in the present paper, as well as the interpretation of the far-infrared spectrum suggests that a non-negligible part of the species is still present as the monomer $AlMe_3$. It is difficult to establish without further experiments to what extent this observation is at variance with the current view exposed in literature[9,10] that this species is highly associated (in dimeric form). We suggest that further experiments will be necessary, involving a careful study of the effect of temperature, concentration, and nature of the solvent.

3.4.2. Aluminum Ethyl Species. Experimental and calculated far-infrared spectra for aluminum ethyl compounds have been collected in Figures 6−8. Again focusing on the range below 650 cm^{-1}, the agreement between the calculated and experimental spectrum for $Al_2Et_4Cl_2$ is simply very satisfactory, for both frequencies and (relative) intensities. Next we discuss the $Al_2Et_3Cl(Cl_2)$ species. Also for this species the correspondence between the experimental and the calculated far-infrared spectrum is pretty satisfactory. The calculated bands at 344, 417, and 504 cm^{-1} match well with the experimentally observed spectrum, while the weaker absorption band calculated at 559 cm^{-1} and observed at 548 cm^{-1} is also recovered. The structure in the band centered around 325 cm^{-1} in the experimental spectrum suggests that contribitions arising from weaker bands calculated at 282 and 360 cm^{-1} appear as shoulders to the strong absorption observed at 325 cm^{-1} and calculated at 344 cm^{-1}.

When we compare the calculated spectra for the various $Al_2Et_2Cl_2(Cl_2)$ species to the experimental spectrum, the fact that the three relatively strong absorption bands appear at almost identical calculated frequencies implies that we will have to focus on relative intensities in order to assign the experimental spectrum to one or more of the configurations. The observation from the experimental spectrum that the high-frequency absorption band around 480 cm^{-1} is the strongest of these three implies that at least the Al_2Et_2-1,2-$Cl_2(Cl_2)$ or the Al_2Et_2-1,4-$Cl_2(Cl_2)$ is present. We also have to take care not to be misled by peak intensities in the experimental spectrum alone, but we must keep in mind that calculated intensities have to be compared to integrated experimental intensities. This makes the experimental band near 320 cm^{-1} of the same intensity as the band observed experimentally close to 400 cm^{-1}. It might seem that the Al_2Et_2-1,2-$Cl_2(Cl_2)$ species is now a likely candidate to be assigned. However, the strong calculated band near 620 cm^{-1} is not recovered in the experimental spectrum with similar intensity. Moreover, the relative energies corroborated from our calculations indicate that the Al_2Et_2-1,2-$Cl_2(Cl_2)$ species is clearly less stable in comparison to Al_2Et_2-1,3-$Cl_2(Cl_2)$ and Al_2Et_2-1,4-$Cl_2(Cl_2)$. Noticing that the calculated energy difference between the latter two species is only 0.6 kcal/mol, suggesting that at room temperature 25% of the species may be present as Al_2Et_2-1,3-$Cl_2(Cl_2)$ and 75% as Al_2Et_2-1,4-$Cl_2(Cl_2)$, the experimental spectrum (frequencies and intensities) can be nicely interpreted as a mixture of these two species. Please note the shoulders at 345 and 525 cm^{-1} in the experimental spectrum, which are also seen as bands in the simulated spectrum of Al_2Et_2-1,3-$Cl_2(Cl_2)$.

4. Conclusions

The aim of this study was to investigate the feasibility of a combined experimental/computational approach to elucidate the structure of active sites in catalysts. The experimental part is formed by far-infrared spectral data which are sensitive to the metal−ligand bond, while the computational part comprises quantum mechanical calculations including energy minimization of the molecular structures and the calculation of the vibrational frequencies and infrared intensities. The present work is an initial study with some members of the family of aluminumalkyl species taken as a test case.

The agreement between experimental and Hartree−Fock-calculated far-infrared spectra is found very satisfactory. From the comparison of these two sets of data, it is concluded that different aluminum alkyl species may be uniquely identified on basis of their far-infrared spectrum, assuming both vibrational frequencies and infrared intensities are considered. This result seems to hold promise for further elucidation of the long-debated structure of the active sites in, e.g., Ziegler−Natta catalysis, which will be the subject of future investigations.

The far-infrared spectra suggest, in agreement with the relative energies evaluated in the present study, that methyl-bridged dimer species such as Al_2Me_6 are much less stable than their chloro-bridged equivalents. This observation is in agreement with experimental findings at low concentration and high temperature.

Acknowledgment. Marjel van den Boer is gratefully acknowledged for useful discussions and for critically reading the manuscript. The management of DSM Research is acknowledged for their permission to publish this work.

Supporting Information Available: Table 1 listing minimum energies for the monomer aluminum alkyl/chloride species, Table 2 listing minimum energies for the dimer aluminum methyl/chloride species, Table 3 listing minimum energies for the dimer aluminum ethyl/chloride species (3 pages). Ordering information is given on any current masthead.

References and Notes

(1) *Macromolecular Symposia*; Tritto, I., Giannini, U., Eds.; Hüthig and Wepf Verlag, Heidelberg, 1995; Vol. 89 (Stereospecific Polymerization).

(2) Cossee, P. *J. Catal.* **1964**, *3*, 80−88.

(3) Weiss, H.; Ehrig, M.; Ahlrichs, R. *J. Am. Chem. Soc.* **1994**, *116*, 4919.

(4) Lohrenz, J. C. W.; Woo, T. K.; Ziegler, T. *J. Am. Chem. Soc.* **1995**, *117*, 12793.

(5) Meier, R. J.; VanDoremaele, G. H. J.; Iarlori, S.; Buda, F. *J. Am. Chem. Soc.* **1994**, *116*, 7274.

(6) Iarlori, S.; Buda, F.; Meier, R. J.; VanDoremaele, G. H. J. *Mol. Phys.* **1996**, *87*, 801.

(7) Brookhart,M.; Green,M. L. H. *J. Organomet. Chem.* **1983**, *250*, 395−408.

(8) Jensen, V. R.; Børve, K. J.; Westberg, N.; Ystenes, M *Organometallics* **1995**, *14*, 4349.

(9) Crompton, T. R. *Analysis of Organoaluminum and Organozinc Compounds*; Pergamon Press: Oxford, 1968.

(10) Mole, T.; Jeffery, E. A. *Organoaluminum Compounds*; Elsevier Publishing Company: Amsterdam, 1972; p 94 and references therein.

(11) Smith, M. B. *J. Phys. Chem.* **1967**, *71*, 364.

(12) Almenningen, A.; Halvorsen, S.; Haaland, A. *J. Chem. Soc., Chem. Commun.* **1969**, 644.

(13) Henrickson, C. H.; Eyman, D. P. *Inorg. Chem.* **1967**, *6*, 1461.

(14) Hoffmann, E. G. *Zeitschrift für Elektrochemie* **1960**, *Bd. 64*, 616.

(15) Onishi, T.; Shimanouchi, T. *Spectrochim. Acta* **1964**, *20*, 325.

(16) Molnár, J.; Marsden, C. J.; Hargittai, M. *J. Phys. Chem.* **1995** *99*, 9062.

(17) Frisch, M. J.; Trucks, G. W.; Schlegel, H. B.; Gill, P. M. W.; Johnson, B. G.; Robb, M. A.; Cheeseman, J. R.; Keith, T.; Petersson, G. A.; Montgomery, J. A.; Raghavachari, K.; Al-Laham, M. A.; Zakrzewski, V. G.; Ortiz, J. V.; Foresman, J. B.; Cioslowski, J.; Stefanov, B. B.; Nanayakkara, A.; Challacombe, M.; Peng, C. Y.; Ayala, P. Y.; Chen, W.; Wong, M. W.; Andres, J. L.; Replogle, E. S.; Gomperts, R.; Martin, R. L.; Fox, D. J.; Binkley, J. S.; Defrees, D. J.; Baker, J.; Stewart, J. J. P.; Head-Gordon, M.; Gonzalez, C.; Pople, J. A. *Gaussian 94*; Gaussian, Inc.: Pittsburgh, PA, 1994.

(18) Car, R.; Parrinello, M. *Phys. Rev. Lett.* **1985**, *55*, 2471−2474.

(19) Perdew, J. P.; Zunger, A. *Phys. Rev.* **1981**, *B23*, 5048−5079.

(20) Perdew, J. P. *Phys. Rev.* **1986**, *B33*, 8822.

(21) Becke, A. *J. Chem.Phys.* **1992**, *96*, 2155.

(22) Vanderbilt, D. *Phys. Rev.* **1990**, *B41*, 7892−7895.

(23) Bachelet, G. B.; Hamann, D. R.; Schlüter, M. *Phys. Rev.* **1982**, *B26*, 4199.

(24) Coussens, B. B.; Buda, F.; Oevering, H.; Meier, R. J. Submitted for publication.

(25) Lewis, P. H.; Rundle, R. E. *J. Chem. Phys.* **1953**, *21*, 986.

(26) Vranka, R. G.; Amma, E. L. *J. Am. Chem. Soc.* **1967**, *89*, 3121.

(27) Vilkov, L. V.; Mastryukov, V. S.; Sadova, N. I. *Determination of the Geometrical Structure of Free Molecules*; Mir Publishers; Moscow, 1983.

(28) Klemperer, W. *J. Chem. Phys.* **1956**, *24*, 353.

(29) Groenewege, M. P. *Z. Phys. Chem., Neue Folge* **1958**, *18*, 147.

(30) Van der Kelen, G. P.; Herman, M. A. *Bull. Soc. Chim. Belg.* **1956**, *65*, 362.

(31) It has been suggested, see Crompton[10] (page 287), that van der Kelen's material was heavily contaminated by aluminum sesquichloride, $Me_3Al_2Cl_3$.